Spectral Characterization, Photophysics, and Photochemistry of the Four Stereoisomers of 1-(2-anthryl)-4-phenyl-1,3-butadiene

A. Spalletti,[†] G. Bartocci,[†] G. Galiazzo,[‡] A. Macchioni,[†] and U. Mazzucato*,[†]

Dipartimento di Chimica, Università di Perugia, 06123 Perugia, Italy, and Dipartimento di Chimica Organica, Università di Padova, 35131 Padova, Italy

Received: September 1, 1999

Using a synthetic strategy, based on retention of stereochemistry in the reagent cinnamaldehyde, the four geometrical isomers of 1-(2-anthryl)-4-phenyl-1,3-butadiene were obtained and chromatographically purified. Their structures were established by optical and nuclear magnetic spectrometry and confirmed by their photochemical behavior. Their excited state properties were investigated by stationary and pulsed fluorimetric techniques and by laser flash photolysis. This paper reports the spectral characterization of the four isomers and the photophysical and photochemical parameters obtained by irradiation in a nonpolar solvent at different temperatures. The important contribution of adiabatic pathways in the photoisomerization mechanism and the role of an upper excited singlet state in the relaxation properties are discussed. Indication of the presence of at least two conformers was obtained only when exciting at the extreme red onset region of the absorption spectrum.

Introduction

The photophysics and photochemistry of diarylethenes and diarylpolyenes have been the subject of wide investigation in the past decades. *E*-stilbene (S) has been usually taken as a useful prototype to understand the excited state behavior of other diarylolefins.[1] For many years asymmetric analogues of S, where a phenyl group was replaced by larger polycyclic aromatic groups, such as naphthyl, phenanthryl, anthryl, etc., have been studied in our laboratory. These groups were found to have a strong effect on the relaxation pathways of the lowest excited singlet state produced after excitation, generally leading to a decrease in the reactive deactivation and an increase in the radiative one and opening the triplet pathway to isomerization.[2]

The photophysics and photochemistry of *all-E*-α,*ω*-diphenylpolyenes (DPhP) have also been extensively studied by both theoretical and experimental approaches.[1,3] Most interest lies in their role as models for conformational properties and photoisomerization reactions about a polyene double bond in the biological functions of proteins.[4] Particular attention has been given to the ordering of the first excited states of A_g and B_u character which is correlated with the length of the polyene chain and can explain an excited state behavior quite different from that of S.

Diphenylbutadiene (DPhB) and diphenylhexatriene (DPhH) have been particularly investigated.[1,3] Much less is known about the corresponding asymmetric compounds where a phenyl group is replaced by a larger polycyclic group. Along the lines of our previous results on the corresponding ethene derivatives[2] and more recent results on some *all-E*-α,*ω*-dithienylpolyenes,[5] we recently turned to the study of some asymmetric diarylbutadienes. The first compound examined was the 2-anthryl derivative, 1-(2-anthryl)-4-phenyl-1,3-butadiene (2AnPhB). This is a complicated system due to the presence of four stereoisomers (EE, EZ, ZE, and ZZ) and of possible conformational equilibria[1b,6] in solution due to *s*-trans, *s*-cis rotamerism about the single bonds of the polyene chain. In principle, the 2-anthryl group could add the further complication of the hindered rotation of the anthryl group around the single bond with the polyene moiety, deeply investigated in our and other laboratories for the corresponding ethene derivatives, styrylanthracenes (*n*-StAn, with $n = 1$ and 2).[7,8]

Unlike S, where $S_1 \rightarrow T_1$ intersystem crossing (ISC) and $S_1 \rightarrow S_0$ internal conversion (IC) are negligible, so that fluorescence and internal rotation in S_1 are strongly coupled, the longer chain analogues can relax through nonradiative pathways in addition to the radiative and reactive ones. This is particularly true for the anthryl derivatives where the polycyclic group is expected to induce a nonnegligible triplet yield.[7a,9]

Using a synthetic route, based on the preserved configuration of the starting aldehyde, as used, e.g., for the synthesis of cis−trans isomeric carotenoids and vitamin A derivatives,[10] the four geometrical isomers of 2AnPhB were obtained and chromatographically purified. Their characterization by optical and nuclear magnetic spectrometry is described here together with results concerning their photophysical and photochemical properties.

Experimental Section

Absorption, Emission, and Photochemical Measurements. Most measurements were carried out in a mixture of methylcyclohexane/3-methylpentane (MCH/3MP, 9/1, v/v), some others in cyclohexane (CH), acetonitrile (MeCN), and benzene. All solvents were from Fluka.

The absorption measurements were carried out with a Perkin-Elmer Lambda 16 spectrophotometer.

The fluorescence spectra were measured on a SPEX Fluorolog-2 model 1680 spectrofluorimeter. The emission quantum yields were determined using 9,l0-diphenylanthracene in CH

* To whom correspondence should be addressed. E-mail: mazzucato@phch.chm.unipg.it.
[†] Università di Perugia.
[‡] Università di Padova.

10.1021/jp9931096 CCC: $18.00
Published on Web 10/27/1999

SCHEME 1

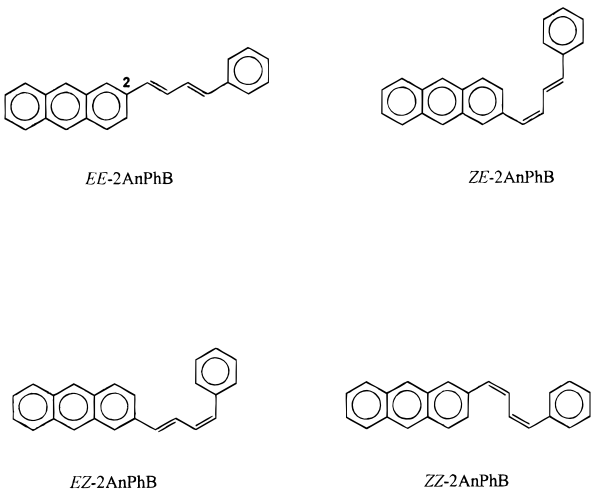

as standard ($\phi_F = 0.90$[11]). The values reported in the tables are averages of at least three independent experiments with a mean deviation of ca. 5%. The fluorescence lifetimes (τ_F, mean deviation of three independent experiments, ca. 7%) were measured with both an Edinburgh Instrument 199S spectrofluorometer (using the single photon counting method) and a SPEX Fluorolog-τ2 system (using the phase modulation technique).

For photochemical measurements, a 150 W high-pressure xenon lamp coupled with a monochromator was used. The photoisomerization quantum yields, measured by use of ferrioxalate actinometry, are averages of at least three independent experiments with a mean deviation of ca. 10%. The reactions were monitored by absorption spectrometry and by HPLC. For chromatographic measurements, a Waters apparatus was used equipped with a Simmetry C_{18} column (4.6 × 200 mm) and a UV detector coupled with an integrator (eluent: MeCN/H_2O mixtures).

The triplet properties were measured by laser flash photolysis at 355 nm using the third harmonic of a Continuum (Surelite II) Nd:YAG laser.

For all experiments the solutions were deoxygenated by purging with nitrogen. A cryostat (Oxford Instruments DN 1704) was used to control the temperature in the 77−354 K range.

Preparation of the Four 2AnPhB Stereoisomers. The compounds investigated (see Scheme 1) were prepared by the Wittig reaction between *E*- and *Z*- (freshly prepared) cinnamaldehyde (CA) and 2-(methylene-triphenylphosphonium-bromide)-anthracene, which generally gives a mixture of two stereoisomers. The synthetic strategy followed for the preparation of the two mixed stereoisomers (ZE, namely in cis geometry at the double bond adjacent to the anthryl group, and EZ, namely in cis geometry at the second double bond, adjacent to the phenyl group) was based on the idea that the nature of the products depends on the stereochemistry of the starting CA. Due to the relatively low temperature of the Wittig reaction, the reagent is expected to preserve its geometrical configuration during the synthesis, as reported for related compounds.[10] Therefore, starting from *E*- and *Z*-CA, one should obtain primarily ZE and EZ compounds, respectively. The products obtained by this procedure confirmed such expectation. In fact, starting from *E*-CA, the EE isomer was the major product in the synthetic mixtures, and there were smaller amounts of the ZE isomer. On the other hand, use of quasipure *Z*-CA,[12] whose preparation is described in the Supporting Information, led to a mixture of EZ and ZZ compounds.

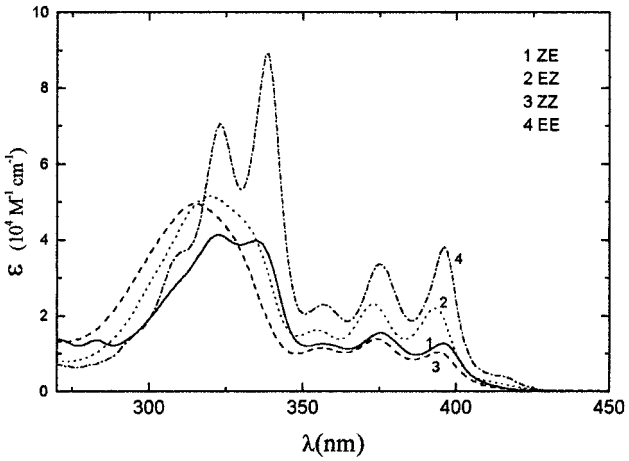

Figure 1. Absorption spectra of the four stereoisomers of 2AnPhB in MCH/3MP at room temperature.

The assignment of the four 2AnPhB stereoisomers was based on, in addition to the expectation derived from the synthetic route, their spectral and photochemical behavior and particularly on nuclear magnetic resonance spectrometry.

Characterization of the 2AnPhB Stereoisomers by NMR. One- and two-dimensional ^{1}H NMR spectra were measured on Bruker AC 200 and DMX 500 spectrometers using TMS as reference. The samples were prepared under a red light dissolving about 2 mg of compound in 0.5 cm^3 of deuterated dichloromethane (CD_2Cl_2). Two-dimensional ^{1}H-DQFCOSY[13] and ^{1}H-phase sensitive NOESY[14] spectra (mixing time 800 ms) were measured as described elsewhere.[15] The distinction between the ZZ and EE isomers was achieved by the values of the ^3J olefinic coupling constants[16] while the other two isomers (EZ and ZE) were discriminated by ^{1}H-NOESY NMR spectra (see Supporting Information).

Results and Discussion

Characterization of the 2AnPhB Stereoisomers by Absorption and Emission Spectroscopy. Comparison of the spectral data of *all-E*-2AnPhB with those of the corresponding ethene derivative, *E*-2-styrylanthracene (*E*-2-StAn),[7a] shows a substantial red-shift reflecting the increase in conjugation which stabilizes the excited states more than the ground state in the longer chain compounds.

Figure 1 shows the absorption spectra of the four stereoisomers of 2AnPhB in MCH/3MP at room temperature. They show the presence of two main bands. The first one in the 350−410 nm region has a well resolved vibronic structure with a progression of ca. 1450 cm^{-1}, as previously observed for *E*-2-StAn, which points to an anthracenic nature of the excited singlet state involved.[7a] The second one, more intense, probably of styrenic type, is localized in the 280−350 nm region. In addition to these two bands, a weak shoulder, more evident in the absorption spectrum of the EE isomer, is also observed at the onset (∼420 nm) of the spectra. By analogy with *E*-2-StAn,[7] it could be part of the forbidden $S_0 \rightarrow S_1$ transition of the B rotamer, which becomes more evident in the butadiene analogues, probably because of a larger energy gap between the S_1 and S_2 states of ^1L_b and $^1(L_a - B_u)$ nature, respectively. Alternatively, it could correspond to absorption by a different rotamer with relatively low equilibrium population (see below).

Figure 2 shows the absorption, excitation and fluorescence spectra of the EE isomer in MCH/3MP at room temperature. The fluorescence spectrum displays the same vibronic structure

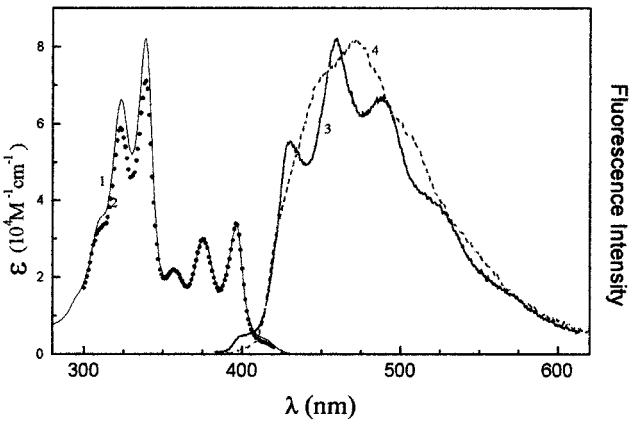

Figure 2. Absorption (1), excitation (2), and fluorescence spectra [$\lambda_{exc} < 405$ nm (3) and $\lambda_{exc} \geq 425$ nm (4)] of *EE*-2AnPhB in MCH/3MP at room temperature.

described above for the absorption spectrum, with $\Delta\bar{\nu} = 1450$ cm^{-1}. These structured spectra indicate a predominance of "quasiplanar" geometries in both the ground and excited states. In principle, conformational equilibria between different geometries,[6] which could derive from the lack of free rotation around the C−C bonds of the chain (as found for DPhPs[1,17−19]) or around the quasisingle bond of the anthryl group with the ethene bridge (as previously found for *E*-2-StAn[7,8]), cannot be excluded in solutions of these molecules. However, the shapes of the fluorescence excitation and emission spectra are practically independent of the emission (λ_{em}) and excitation (λ_{exc}) wavelength (the latter, below 405 nm), respectively. Furthermore, the fluorescence excitation spectrum is practically coincident with the absorption spectrum (see Figure 2). The fluorescence decay is monoexponential and the fluorescence quantum yield is independent of λ_{exc} (see below). These results indicate that the presence of rotamers in the ground and excited states is not easily detectable in fluid solution at room temperature. Nevertheless, by exciting at the red-edge absorption tail with $\lambda_{exc} > 410$ nm, the shape of the emission spectrum drastically changes (then remaining practically independent of λ_{exc} at longer wavelengths, $\lambda_{exc} > 426$ nm; see spectrum 4 of Figure 2) and the fluorescence decay becomes biexponential.

Figure 3 shows the absorption, excitation and fluorescence spectra obtained by excitation of dilute solutions of the other three stereoisomers. The emission spectra were found to be independent of λ_{exc} until 400 nm, and the corresponding excitation spectra to be independent of λ_{em} and almost coincident with the absorption spectra. Only at $\lambda_{exc} > 405$ nm did the emission spectrum of the EZ isomer change its shape, as previously shown for EE. However, in contrast to EE, the spectral shape of the other isomers drastically depends on temperature (see Figure 4). The emission spectra, produced by excitation of the ZE, EZ, and ZZ stereoisomers of 2AnPhB, become more and more similar to that of the EE analogue, by increasing the temperature, thus pointing to involvement of adiabatic isomerization pathways in the singlet manifold, which produce the *all-E* isomer in the excited singlet state (^{1}EE*). Therefore, the measured emission spectra are the superpositions of at least two components, due to the starting excited compound and the photoproduced ^{1}EE* (see below). The true fluorescence spectra of the EZ and ZE isomers at room temperature, shown in Figure 5, were derived by spectral subtraction: the emission spectrum of EE (spectrum 3 of Figure 2), weighted by its abundance (derived from the fluorescence decay curves, see below), was subtracted from the experimental spectrum of the

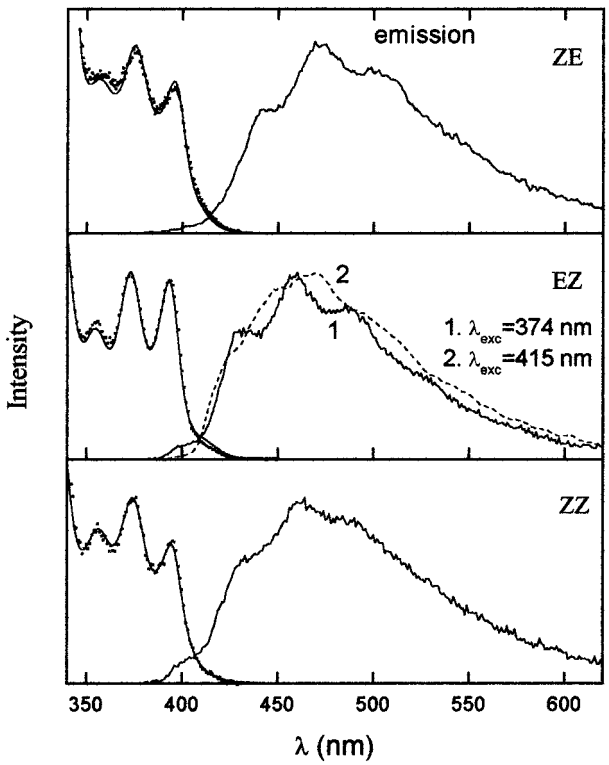

Figure 3. Absorption (full line), excitation (dotted line) and emission spectra obtained by excitation of diluted solutions of the ZE, EZ, and ZZ isomers of 2AnPhB in MCH/3MP.

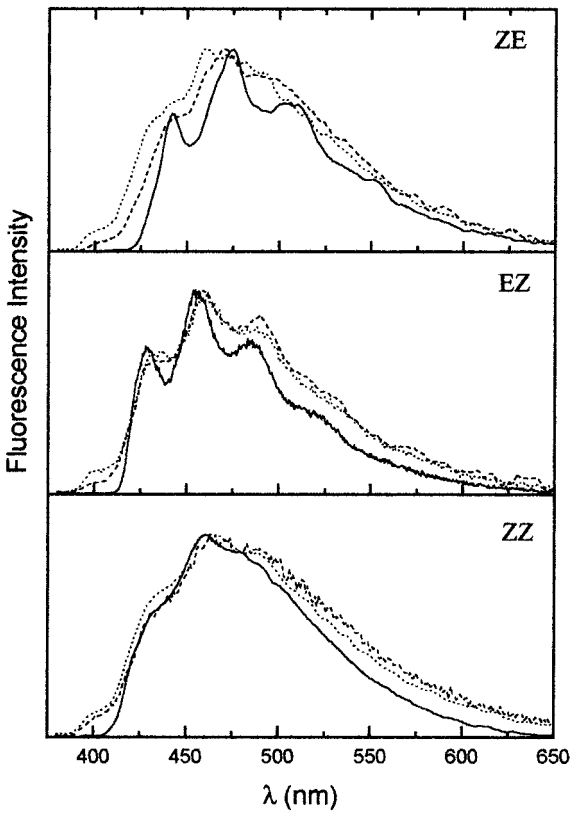

Figure 4. Temperature effect on the fluorescence spectra obtained by excitation of dilute solutions of ZE, EZ, and ZZ isomers of 2AnPhB in MCH/3MP. The spectra are recorded at 77 K for EZ and ZZ, 175 K for ZE (full line), at 293 K (dashed line) and 354 K (dotted line).

conformer mixture. In the case of the ZE isomer, the true emission spectrum was also obtained at 175 K, where the ^{1}ZE* → ^{1}EE* adiabatic process is no longer competitive. The resulting

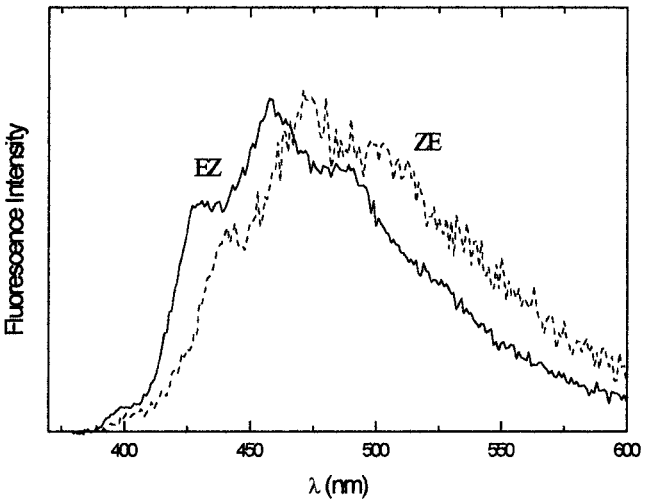

Figure 5. Fluorescence spectra of the EZ and ZE isomers of 2AnPhB in MCH/3MP at room temperature as derived by subtraction of the contribution of the EE isomer (see text).

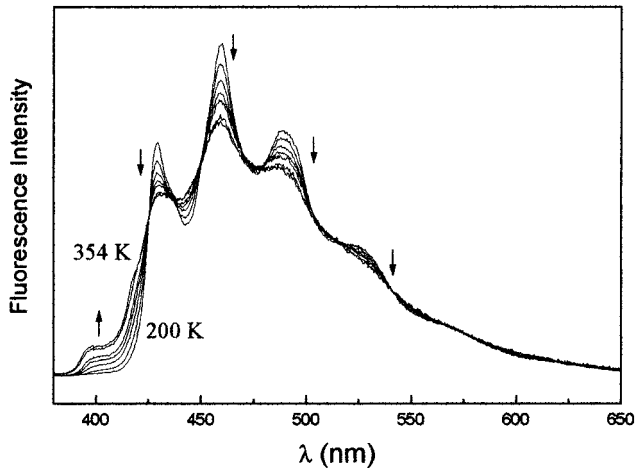

Figure 6. Temperature effect (in the range 200−354 K) on the fluorescence spectra (normalized at unitary area) of *EE*-2AnPhB in MCH/3MP (λ_{exc} = 375 nm).

spectrum is very similar to that obtained at room temperature by spectral subtraction. For the ZZ compound, the true emission spectrum was not isolated, even at low temperature. The broad spectrum obtained at 77 K was not structured and clearly appeared as the sum of different contributions, probably due to adiabatic formation of the other stereoisomers, still operative in rigid matrices.

Emission from an Upper Excited Singlet State in 2AnPhBs. An anomalous emission, analogous to that previously observed for *E*-2-StAn[20,21] and *all-E*-DPhH[1,17,22] was observed in the spectra of the EE, EZ, and ZE stereoisomers of 2AnPhB as a shoulder at ca. 400 nm, whose intensity changed with temperature (see Figure 6) but not with λ_{exc}. It was assigned to a second emissive component of the prevailing B rotamer, which originates from an upper excited state on the basis of the following considerations: (i) the corresponding excitation spectrum recorded at $\lambda_{em} \cong 400$ nm is coincident with that recorded at $\lambda_{em} \cong 430$ nm in correspondence with the 0,0 peak of the $S_1 \rightarrow S_0$ transition; (ii) the intensity ratio $I_{F,2}/I_{F,1}$ between the first two peaks of the fluorescence spectrum ($I_{F,2}$ and $I_{F,1}$ at λ_{em} of 400 and 430 nm, respectively) remains practically constant on changing λ_{exc}; and (iii) the Stokes shift between the absorption peak at 396.5 nm (essentially due to the 0,0 peak of the allowed $S_0 \rightarrow S_2$ transition) and the hypsochromic shoulder of the fluorescence spectrum is very small (ca. 220 cm^{-1}) thus indicating that the two transitions involve the same excited state (S_2). The involvement of the upper excited state S_2 in the photophysics of *E*-1,2-diarylethenes has been recently observed through absorption measurements by picosecond laser flash photolysis.[23]

A quantitative analysis of the anomalous emission was only applied to the EE isomer due to the higher weight of its $S_2 \rightarrow S_0$ transition. For the other isomers, this hypsochromic emission is partially masked by the analogous $S_2 \rightarrow S_0$ emissive component of adiabatically formed ^{1}EE*, whose relative intensity increases with temperature (see below). The decrease in the intensity ratio of the two components with temperature, until the disappearance of the first component below 200 K, indicates that the latter pertains to an emission from S_2 thermally populated from S_1 during its lifetime. The energy difference between the two states, $\Delta E(S_2-S_1)$, was obtained, as in the case of *E*-2-StAn, from plots of ln $I_{F,2}/I_{F,1}$ and of ln [$I_{F,2} \times \tau_F$(293 K)/$\tau_F(T)$] vs $1/T$, because both of these quantities are proportional to the energy gap.[20] The latter equation was used in the form which includes the dependence of the fluorescence lifetime on temperature (see below). An average value of 1110 ± 30 cm^{-1} was derived from the two plots. Moreover, by using eq 1

$$I_{F,2}/I_{F,1} = k_{F,2}/k_{F,1}[S_2]/[S_1] \quad (1)$$

(where the ratio $[S_2]/[S_1]$ corresponds to the Boltzmann factor, $\exp[-\Delta E(S_2-S_1)/RT]$, which gives the fractional contribution of S_2 during the S_1 lifetime), a rate parameter ratio, $k_{F,2}/k_{F,1}$, of 20 was obtained. Values of $\Delta E(S_2-S_1)$ of 1020 and 1100 cm^{-1}, respectively, were also roughly estimated from the fluorescence spectra of the ZE and EZ isomers (Figure 5).

Photophysical and Photochemical Parameters. *EE-2AnPhB.* The radiative process is an important relaxation pathway for the EE isomer in MCH/3MP at room temperature. Its quantum yield (ϕ_F = 0.36) is nearly independent of λ_{exc}. The fluorescence decay is monoexponential at $\lambda_{exc} \leq 400$ nm (τ_F = 67 ns), while, as stated above, it becomes biexponential at longer λ_{exc} because of the presence of a short-lived component ($\tau_{F,A}$ = 32 ns; $\tau_{F,B}$ = 66 ns). By analogy with *E*-2-StAn,[7] we label the species responsible for the short- and longer-lived components A and B, respectively. The short-lived one (see spectrum 4 of Figure 2) has a smaller abundance [%(A) = 24 at 293 K, λ_{exc} = 416 nm and λ_{em} = 470 nm] which markedly increases with temperature [%(A) = 55 at 354 K]. The k_F values, obtained from the ϕ_F/τ_F ratios of the two species ($\phi_{F,A}$ = 0.35, obtained at $\lambda_{exc} \geq 426$ nm, $\phi_{F,B}$ = 0.36 and $\tau_{F,A}$ = 32 ns, $\tau_{F,B}$ = 67 ns) were found to be 11 and 5.4 (10^6 s^{-1}) for A and B, respectively. A comparison with the behavior of *E*-2-StAn[7,8] indicates that the two emission components are due to the two rotamers arising from the hindered rotation of the anthryl group around the quasisingle bond with the carbon atom of the chain. The ϕ_F values of the two rotamers are smaller than those of the ethene derivative, leading to a decrease in k_F for the diene. Greater stabilization of the S_1 state (^1L_b*) relative to S_2 [$^1(L_a - B_u)$*] state of the B rotamer is expected in the diene compound, owing to their different nature, and is confirmed by the comparison between the absorption spectra of the ethene and diene analogues. This increases the energy gap between the two states, as recently found for dithienylbutadienes,[5] thus decreasing their mixing through vibronic coupling. This fact makes the $S_1 \rightarrow S_0$ radiative transition less allowed than in the case of the ethene analogue. The k_F value of the A rotamer decreases by almost 1 order of magnitude relative to that of the *E*-2-StAn(A) rotamer,[7b] thus indicating an inversion in the order of the two lowest

TABLE 1: Temperature Effect on the Fluorescence Quantum Yield and Lifetime of *EE*-2AnPhB in MCH/3MP (λ_{exc} = 375 nm)

T (K)	ϕ_F	τ_F (ns)
354	0.25	58
343	0.26	60
333	0.33	61
313	0.36	64
293	0.36	67

excited singlet states in the diene compound. In the *EE*-2AnPhB-(A) rotamer, the S_1 state assumes a ^1L_b nature and the $S_1 \rightarrow S_0$ radiative transition becomes partially allowed by vibronic coupling with the closely located S_2 state of $L_a - B_u$ nature.

The increase in the $\Delta E(S_2-S_1)$ value for the butadiene derivative, with respect to the ethene analogue, explains the reduced contribution of the $S_2 \rightarrow S_0$ component in the fluorescence spectrum of *EE*-2AnPhB. A radiative rate constant $k_{F,2} = 1.1 \times 10^8\ s^{-1}$, a value which confirms the $(L_a - B_u)$ character of the S_2 state, was obtained from the values of k_F and $k_{F,2}/k_{F,1}$, derived above. The rate parameter of the nonradiative processes (k_{NR}), namely internal conversion (IC) and/or intersystem crossing (ISC), derived from the fluorescence lifetime and quantum yield [$k_{NR} = (1 - \phi_F)/\tau_F$], indicates an increase in the contribution of such deactivation pathways of S_1 for both rotamers of the diene compound in comparison with the analogous ethene. As for the latter,[7a] the EE isomer does not photoisomerize detectably at room temperature, even after a long irradiation time, the electron distribution in the diene chain being such as to induce high torsional barriers at both double bonds.

The triplet behavior of *EE*-2AnPhB was studied by laser flash photolysis at room temperature in a nonpolar solvent. The following parameters were obtained: λ_{max} = 430, 460, 600 and 640 nm, $\tau_T = 11\ \mu s$, and $\phi_{ISC} = 0.05$. As previously found for *E*-2-StAn,[9,24] the relatively long triplet lifetime is due to a high torsional barrier for the internal rotation leading to the perpendicular (P) configuration in the triplet manifold, namely $^3EE^* \rightarrow {}^3EP^*$ (or $^3PE^*$).

In *EE*-DPhB, a smaller triplet yield ($\phi_{ISC} = 0.02$) and a markedly shorter triplet lifetime ($\tau_T = 1.6\ \mu s$) in CH were reported.[25] A longer lifetime for the anthryl derivative, related to a less reactive T_1 state, was also indicated by the fact that no triplet-donor sensitized isomerization to EZ (or ZE) was observed for *EE*-2AnPhB (ϕ_{EZ}^{sens} or $\phi_{ZE}^{sens} \cong 0$), while a high value was reported for DPhB.[25]

The ISC rate constant was evaluated ($k_{ISC} = \phi_{ISC}/\tau_F = 7.5 \times 10^5\ s^{-1}$) from the above triplet parameters. Since the sum ($k_F + k_{ISC}$) is lower than $1/\tau_F$, a contribution of $S_1 \rightarrow S_0$ internal conversion (IC) to the relaxation pathways cannot be excluded, in contrast to what was found for *E*-2-StAn.[7a] An approximate value of $8.8 \times 10^6\ s^{-1}$ was derived for the IC rate constant on the basis of the relationship $k_{IC} = 1/\tau_F - (k_F + k_{ISC})$.

The lifetime and quantum yield of fluorescence are practically independent of temperature up to 310 K. At higher temperatures these emission parameters decrease (see Table 1) and excitation of EE solutions leads to formation of two photoproducts (very probably the EZ and ZE isomers).

These results, which are similar to those previously found for *E*-2-StAn[26] in the same solvent, can be explained on the basis of the fluorescence lifetime. In fact, the small $1/\tau_F = \Sigma k_i$ value ($1.5 \times 10^7\ s^{-1}$), which accounts for the radiative and nonradiative deactivation pathways of S_1, makes the photoreactive pathway observable above room temperature even in the presence of high torsional barriers.

TABLE 2: Fluorescence and Photoisomerization[a] Quantum Yields Obtained by Irradiation of Solutions of *EZ*-, *ZE*-, and *ZZ*-2AnPhB in MCH/3MP at 293 K (λ_{exc} = 375 nm)

compound	$\bar{\phi}_F$	ϕ_{EE}	ϕ_{ZE}	ϕ_{EZ}
ZE-2AnPhB	0.22	0.20		
EZ-2AnPhB	0.29	0.35		
ZZ-2AnPhB	0.19	0.11	0.13	0.036

[a] Subscripts refer to the photoisomerization product.

TABLE 3: Fluorescence Decay Parameters Obtained by Irradiation of Solutions of *EZ*-, *ZE*-, and *ZZ*-2AnPhB in MCH/3MP at Different Excitation and Emission Wavelengths at 293 K[a]

compound	λ_{exc} (nm)	λ_{em} (nm)	$\tau_{F,1}$ (ns)	$\tau_{F,2}$ (ns)	%(1)
ZE-2AnPhB	337	400	24	58	68
	337	480	25	72	85
	358	480	25	68	85
	375	480	23	62	82
EZ-2AnPhB	322	407	19	58	44
	322	440	28	68	57
	375	>380[b]	25	68	50
ZZ-2AnPhB	337	460	17	58	52
	375	460	19	59	56
	375	480	22	58	60

[a] The corresponding weights (%) are also reported. [b] Obtained by phase modulation technique.

EZ, ZE, and ZZ stereoisomers of 2AnPhB. After direct irradiation of dilute deaerated solutions of the EZ, ZE, and ZZ isomers of 2AnPhB in MCH/3MP at room temperature (λ_{exc}= 375 nm), the HPLC analysis showed the formation of one or more geometrical isomers. Specifically for the EZ and ZE isomers, the main photoproduct was EE (see Table 2). Characterization of the diene isomers rests on their HPLC elution times and on UV and NMR spectral data. The appearance of EE during the first irradiation times of ZZ indicates the involvement of one photon−two bond isomerization. Similar results of multiple bond isomerization were previously reported for 2,4-hexadiene,[27] cyano-substituted diphenyl-1,3,5-hexatrienes,[28] *p*-styryl-stilbene,[29] and distyryl-arenes.[30] This process takes place probably through a mechanism involving two consecutive adiabatic processes ($^1ZZ^* \rightarrow {}^1ZE^*$ ($^1EZ^*$) $\rightarrow {}^1EE^* \rightarrow {}^1EE$)[29,30] as indicated by the multicomponent emission from the singlet excited intermediates (see Table 3). The basic requirement for the occurrence of one photon−two bond isomerization is that the process be barrierless or experience small barriers. The isomerization mechanism is then controlled by the relative values of the torsional barriers. No production of cyclic photoproducts was found after irradiation of aerated solutions of the three geometrical isomers of *EE*-2AnPhB.

The three compounds have fluorescence quantum yields of about 0.2−0.3, relatively lower than *Z*-2-StAn ($\phi_F \cong 0.5$).[26,31,32] This suggests that the $S_1 \rightarrow S_0$ IC is a significant deactivation pathway of S_1. The fluorescence decay was found to be multiexponential in MCH/3MP at room temperature. The biexponential treatment gives the following parameters: a longer-lived component, τ_{F2}, assigned to the adiabatically formed $^1EE^*$ on the basis of its emission spectrum and lifetime ($\tau_{F,EE}$ = 67 ns), and a short-lived component (ca. 25 ns), assigned to $^1EZ^*$ or $^1ZE^*$ because of its presence at $\lambda_{exc} < 400$ nm, where the fluorescence decay of $^1EE^*$ is monoexponential. At room temperature, the fluorescence lifetimes of the EZ and ZE isomers are very similar and the contributions of the short-lived components on the total decay are independent of λ_{exc} (see Table 3), thus supporting the hypothesis that the longer-lived $^1EE^*$ component is adiabatically produced.

TABLE 4: Fluorescence Quantum Yield and Lifetime Together with the Weights of the EE Emissive Component on the Total Fluorescence [%(2)] and the Singlet Adiabatic Quantum Yield ($^1\phi_{ad,EE}$) and the Singlet Quantum Yield of Formation of Perpendicular Geometries ($^1\phi_{EP}$ and $^1\phi_{PE}$), Obtained by Irradiation of Solutions of *EZ*- and *ZE*-2AnPhB in MCH/3MP at Different Temperatures (λ_{exc} = 375 nm, λ_{em} = 480 nm)

compound	T (K)	$\bar{\phi}_F$	$\tau_{F,1}$ (ns)	$\tau_{F,2}$ (ns)	%(2)	$^1\phi_{ad,EE}$	$^1\phi_{PE}$[a]	$^1\phi_{EP}$[a]
ZE-2AnPhB	354	0.22	18	57	45	0.40	0.38	
	333	0.22	20	56	36	0.24	0.26	
	313	0.21	23	62	27	0.16	0.19	
	293	0.22	25	68	18	0.11	0.12	
	265	0.23	27	69	10	0.05	0.05	
EZ-2AnPhB	354	0.28	20	64	62	0.69		0.50
	293	0.29	25	68	40	0.32		0.38

[a] Obtained by eqs 3 and 4.

The decay curve, observed after excitation of the ZZ isomer, shows at least two exponentials. In the case of a biexponential deconvolution treatment, we found the τ_F values of 58 and ca. 19 ns, assigned to the final photoproduct EE and a mixture of the EZ and ZE isomers, respectively, on the basis of their intrinsic lifetimes (67, 24 and 22 ns for EE, ZE, and EZ, respectively). The reduction in lifetime, particularly for the EE isomer (67 ns for the pure component, see Table 1), is probably due to the error in the deconvolution procedure when two or three terms with different amplitudes and/or not well separated lifetimes are implied in the decay curves of ZE (or EZ) and ZZ, respectively. However, these deviations can also reflect, at least in part, the effect of variable amounts of residual oxygen in the solutions, particularly for the long-lived EE isomer. A third, shorter-lived component (6 ns), with a very low weight on the total decay (ca. 4%), was resolved with the use of a three-exponential treatment of the decay curve by global analysis in the phase modulation experiments. It was tentatively assigned to a weak intrinsic emission of ZZ itself.

The experimental $\bar{\phi}_F$ values of Table 2 are the sum of the contributions from the species directly excited and from their isomeric photoproducts adiabatically formed in the singlet manifold. A quantitative fluorescence analysis was carried out for the EZ and ZE isomers to obtain their S_1 properties. If the fluorescence decay is observed at 480 nm, which is practically an emission maximum for all isomers, the ratio of the fluorescence intensities can be reasonably replaced by that of the fluorescence quantum yields, considering that these compounds have similar emission spectra (see Figures 2 and 5). Therefore, with the use of the relationship $\phi_{F,EZ} = \%(EZ) \times \bar{\phi}_F$, or the analogous one for ZE, fluorescence quantum yields of 0.17 and 0.18 were obtained for EZ and ZE, respectively, in MCH/3MP at room temperature.

Using the fluorescence quantum yields and decay parameters as a function of temperature (Table 4), the quantum yield for the adiabatic isomerization in S_1, $^1\phi_{ad,EE}$, could be derived at any temperature from

$$^1\phi_{ad,EE} = (\bar{\phi}_F - \phi_{F,EZ})/\phi_{F,EE} \qquad (2)$$

or from the analogous equation with ZE instead of EZ. The results in MCH/3MP at room temperature are reported in Table 4. They show that (i) the adiabatic process, leading to EE, is an important deactivation pathway of S_1, (ii) $^1\phi_{ad,EE}$ has a larger value for EZ compared to ZE, in agreement with the spectral results (the fluorescence spectrum, obtained by excitation of EZ, is the most similar to that of EE), and (iii) at room temperature, the ZE → EE photoisomerization only partially proceeds through a singlet adiabatic mechanism, because the $^1\phi_{ad,EE}$ value, derived by the use of eq 2, is lower than the overall quantum yield of EE formation, ϕ_{EE} (see Table 2). Therefore, the involvement of an additional diabatic singlet mechanism and/or a triplet pathway cannot be excluded in the photoreactive process of the ZE isomer (for a final interpretation, see below).

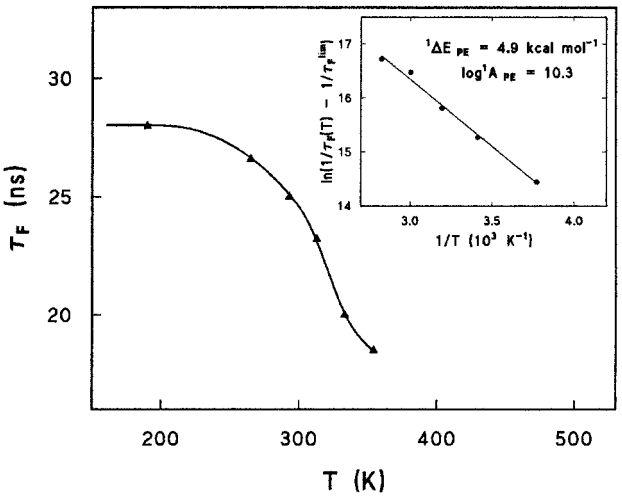

Figure 7. Fluorescence lifetime of *ZE*-2AnPhB in MCH/3MP as a function of temperature. The inset shows the corresponding Arrhenius plot according to eq 3.

The dependencies of the lifetimes and $^1\phi_{ad,EE}$ values of the EZ and ZE isomers on temperature (see Table 4) indicate that the photoreactive pathway is an activated process. Assuming all other decay pathways of S_1 are temperature independent, by use of the Arrhenius-type equation for the temperature effect on τ_F of the ZE isomer

$$\ln(1/\tau_F(T) - 1/\tau_F^{lim}) = \ln {}^1A_{PE} - {}^1\Delta E_{PE}/RT \qquad (3)$$

a limiting value for the frequency factor and the energy barrier of the ^{1}ZE* → ^{1}PE* process was estimated. A lifetime of 28 ns was measured at low temperatures where the reactive activated process is inhibited (τ_F^{lim}). The Arrhenius parameters $^1A_{PE}$ = 2.2 10^{10} s^{-1} and $^1\Delta E_{PE}$ = 4.9 kcal mol^{-1} were derived from the plot in Figure 7. In the case of EZ, the parameters $^1A_{EP}$ = 2.8 10^8 s^{-1} and $^1\Delta E_{EP}$ = 1.7 kcal mol^{-1} were roughly estimated from the values at two temperatures only and from a τ_F^{lim} value of 42 ns.

The torsional barriers for the process leading to the perpendicular configuration, ^{1}ZE* → ^{1}PE* or ^{1}EZ* → ^{1}EP*, are quite low, particularly for EZ, thus explaining the presence of the radiative component of ^{1}EE*, adiabatically formed, even at rather low temperatures (see Figure 4).

The frequency factor values (<10^{11} s^{-1}) are much lower than those expected for a spin-allowed process (10^{12} to 10^{13} s^{-1}). A tentative explanation for this anomalous behavior can be based on the hypothesis that coupling of solute−solvent motions, in the particular case of these compounds in cis geometry, which have flat curvature of the torsional barriers, could cause recrossing of the transition state of the reacting system (^{1}EP* or ^{1}PE*), thus reducing the percentage of molecules moving along the reaction coordinate (transmission coefficient smaller than unity).[33] Such explanation was proposed, e.g., for DPhB[33a] and 2-vinylanthracene.[33b] However, taking into account the uncertainty in the frequency factors reported above, we conclude that further studies of the temperature and solvent effects (in

isoviscosity conditions) are needed before reaching a less speculative interpretation.

From the Arrhenius parameters, the quantum yield values of the ^{1}ZE*→^{1}PE* process ($^1\phi_{PE}$) as a function of temperature were derived by the use of the equation

$$^1\phi_{PE}(T) = {}^1k_{PE}(T)\tau_F(T) = [{}^1A_{PE}\exp(-{}^1\Delta E_{PE}/RT)]\tau_F(T) \quad (4)$$

The $^1\phi_{PE}$ values thus obtained as a function of temperature are shown in Table 4. They are practically equal to the $^1\phi_{ad,EE}$ values, derived by the use of eq 2 at the corresponding temperatures, thus indicating that the involvement of a diabatic singlet pathway must be excluded. However, the experimental quantum yield of the photoreactive ZE → EE process (ϕ_{EE}) is higher than $^1\phi_{PE}$, pointing to a mixed singlet and triplet adiabatic mechanism.

In the case of the EZ isomer, the ϕ_{EE} values at two temperatures ($\phi_{EE} = 0.55$ at 354 K), are roughly similar to both the $^1\phi_{ad,EE}$ and $^1\phi_{EP}$ derived by eqs 2 and 4, respectively, thus indicating that the torsional process proceeds through an adiabatic singlet mechanism only.

For the ZE isomer, the yield of EE formation can be expressed as the sum of the singlet ($^1\phi_{EE}$) and triplet ($^3\phi_{EE}$) contributions

$$\phi_{EE} = {}^1\phi_{EE} + {}^3\phi_{EE} \quad (5)$$

By eq 5, a value of 0.08 was derived for $^3\phi_{EE}$ at 293 K (see Tables 2 and 4). Since $^3\phi_{EE} = \phi_{ISC} \times \phi_{EE}^{sens}$, eq 5 can be expressed as

$$\phi_{EE} = {}^1\phi_{EE} + k_{ISC}\tau_F\,\phi_{EE}^{sens} \quad (6)$$

The biacetyl sensitized photoisomerization has a quantum yield, ϕ_{EE}^{sens}, of about 1.0 in benzene at room temperature at the same ZE concentration used in the direct irradiation (about 8×10^{-5} M). A k_{ISC} value of 3.3×10^6 s^{-1} was derived for the ZE isomer in diluted solutions at room temperature.

At higher concentrations, ϕ_{EE}^{sens} assumes values > 1 (1.8 and 2 at 5.5×10^{-4} and 7.3×10^{-4} M, respectively) which are due to the chain mechanism implying energy transfer from ^{3}EE*, adiabatically formed, to the ground-state ZE, in agreement with previous results found for other Z isomers of *n*-StAn.[34−38]

A similar concentration effect was observed also on the direct isomerization quantum yield for which the values of 0.20 and 0.29 were measured in benzene solutions, at 1.4×10^{-4} and 7.1×10^{-4} M, respectively. This result confirms the involvement of a triplet adiabatic mechanism in the photoreactive process of the ZE isomer. In fact, the experimental ϕ_{EE} value obtained at the high concentration (0.29) is in very good agreement with that derived (0.28) by the use of eq 6 at the same concentration.

Kinetic Parameters. The fluorescence quantum yields and lifetimes are reported in Table 5 together with the derived rate parameters for the radiative (k_F) and nonradiative (k_{ISC}, $^1k_{ad,EE}$ and k_{IC}) processes of the S_1 deactivation of three 2AnPhB geometrical isomers and of *E*-2-StAn, for comparison, in nonpolar fluid solutions at 293 K. For the ZZ isomer, a quantitative analysis of the photophysical and photochemical behavior was not carried out because of its complexity. The high rates of its parallel adiabatic processes make derivation of the photophysical parameters practically impossible.

The $S_1 \rightarrow S_0$ IC rate constant, k_{IC}, was derived by use of the equation

$$k_{IC} = 1/\tau_F - (k_F + k_{ISC} + {}^1k_{ad,EE}) \quad (7)$$

TABLE 5: Photophysical and Kinetic Parameters of the 2AnPhB Isomers and *E*-2-StAn (B Rotamer) for Comparison (together with the Energy Gap between the S_1 and S_2 States) in MCH/3MP at 293 K

parameter	E[a]	EE	ZE	EZ
ϕ_F	0.64[b]	0.36	0.18	0.17
τ_F (ns)	65	67	24	25
ϕ_{ISC}	0.12[c]	0.05[d]	0.08	<0.01
ϕ_{ISO}	0.003	<0.001	0.20	0.35
ϕ_{IC}	0.24	0.59	0.62	0.48
$k_{F,1}$ (10^6 s^{-1})	7.7[b]	5.4	7.5	6.8
$k_{F,2}$ (10^8 s^{-1})	2.3 (2.3)[e]	1.1 (3.5)[e]	(1.7)[e]	(2.5)[e]
k_{ISC} (10^6 s^{-1})	1.9	0.75	3.3	<0.4
k_{IC} (10^6 s^{-1})	3.7	8.8	26	19
$^1k_{ad,EE}$ (10^6 s^{-1})			4.4	14
ΔE (S_2-S_1) (cm^{-1})	800	1110	1020[f]	1100[f]

[a] From ref 26. [b] Calculated at low temperature. [c] From ref 9. [d] In benzene. [e] k_F^0 values, calculated with the use of eq 8. [f] From fluorescence spectral data.

Contrary to *E*-2-StAn, whose S_1 state decays almost exclusively by the radiative channel,[2] the main deactivation pathways of the S_1 state of the butadiene analogues are the radiative and the nonradiative and nonreactive (ISC and/or IC) processes. As stated above, the two lowest excited singlet states of "anthracene-like" nature are different in character, namely ^1L_b and $^1(L_a - B_u)$ for S_1 and S_2, respectively, as shown by the k_F values. The $S_1 \rightarrow S_0$ forbidden transition becomes partially allowed by vibronic coupling of S_1 with S_2.[39] As a consequence, its oscillator strength markedly depends on the energy gap between the two lowest excited singlet states.

The presence of the butadiene chain causes a preferential stabilization of S_1, because of its ^1L_b nature, as observed in polyenes,[1a] diphenylpolyenes,[1a] and dithienylpolyenes.[5,40] Therefore, it gives rise to a larger energy gap between S_1 and S_2, a lower k_F value, and a much weaker $S_2 \rightarrow S_0$ emissive component in *EE*-2AnPhB.

For comparison, the radiative rate constants, obtained by use of the modified Strickler−Berg relationship,[41] are reported in Table 5 (values in parentheses):

$$k_F^0 = (\tau_F^0)^{-1} = 2.88 \times 10^{-9}\,\bar{\nu}_{0,0}^{\,2}\,n_s^{\,2}\int \epsilon(\bar{\nu})\,d\bar{\nu} \quad (8)$$

where $\bar{\nu}_{0,0}$ is the 0,0 component of the $S_0 \rightarrow S_2$ allowed transition, which is considered to be mainly responsible for the absorption. Table 5 shows how the k_F^0 values are in reasonable agreement with those derived by the analysis of the "anomalous emission" from an upper (S_2) excited singlet state ($k_{F,2}$). Moreover, the k_{IC} values of EE, ZE, and EZ are much larger than that of the ethene analogue, thus indicating IC as a significant deactivation channel for the butadiene derivatives.

The fast radiationless decay of 2AnPhBs through IC could be due to two effective vibrational modes acting as coupling modes between S_1 and S_0, namely the Franck−Condon active C=C stretching vibration and an out-of-plane torsional mode. The C=C stretching acts both as promoting and accepting mode and it should dominate the radiationless decay in *E*-2-StAn due to its more planar configuration in S_1. The torsional mode can act as an additional accepting mode in the decay of S_1 with a strongly out-of-plane distorted configuration, as in the case of the butadiene analogues.[3d] The participation of the out-of-plane mode increases the IC rate up to about 1 order of magnitude, as found for butadiene.[3d] Furthermore, the lower S_1-S_0 energy gap (ca. 500 cm^{-1}) of 2AnPhBs with respect to that of *E*-2-StAn can enhance the IC process.

In the mixed isomers, EZ and ZE, both ϕ_F and τ_F decrease, relative to EE, in agreement with the occurrence of a significant activated process in S_1, which produces EE mainly by the adiabatic mechanism. This reactive process is an important deactivation pathway, particularly for EZ, in agreement with a smaller torsional barrier, as previously reported for *Z*-2-StAn.[26,31,32]

Conclusions

The spectral characterization of the four stereoisomers of 2AnPhB, prepared by the Wittig reaction, and the study of their photophysics and photochemistry allowed us to obtain a general understanding of the competition of the relaxation processes of their lowest excited states and to compare these results with those previously obtained for the ethene analogue[7,8] and diphenylbutadiene.[1,3] There are several similarities in the behavior of these compounds, but also some important differences. The peculiar effect of the anthryl group on the photobehavior of the dienes investigated, when compared with the phenyl analogues, concerns the photoisomerization mechanism which resembles that reported for the short-chain analogue, 2-StAn.[7,8] The low S_1 and T_1 energies of the anthryl group leads to a high torsional barrier for intramolecular rotation of both *all*-trans geometries, ^{1}EE* and ^{3}EE*, which practically do not isomerize, at least at room temperature. On the other hand, the other stereoisomers, with one or both double bonds in cis geometries, do not experience a deep minimum at 90°, after twisting, but a very shallow minimum or even a saddle point, which produces a change in the isomerization pathway, from the prevalent diabatic mechanism of DPhB to the adiabatic one of these anthryl derivatives, toward excited species in transoid geometries.

The anthryl group also affects the triplet yield, which increases with respect to the corresponding phenyl analogues. However, the photoreaction proceeds only in the cis to trans direction ("one way") through a singlet (in the case of EZ) or mixed (singlet + triplet) (for ZE) mechanism.

A decrease in the efficiency of the radiative relaxation and an increase in the nonradiative pathways were observed for these dienes with respect to 2-StAn. A contribution of IC, essentially absent in the ethene derivative, becomes substantial in the EZ and ZE isomers and may be important for ZZ together with the reactive pathway.

This research work allowed the emission from an upper excited singlet state and the role of conformers in solutions of 2AnPhB to be discussed, even if a more detailed description of these aspects deserves a further study.

Acknowledgment. This work was performed with financial support from the Italian Consiglio Nazionale delle Ricerche and the Ministero per l'Università e la Ricerca Scientifica e Tecnologica (Progetti Nazionali Interuniversitari). The authors are grateful to D. Pannacci for his technical assistance.

Supporting Information Available: A more detailed description of the synthetic work for the four isomers of 1-(2-anthryl)-4-phenyl-1,3-butadiene (2 pages). A list of ^{1}H NMR data useful for the characterization of the four isomers of 1-(2-anthryl)-4-phenyl-1,3-butadiene (4 pages). A Table containing the fluorimetric parameters of *EE*-2AnPhB as a function of λ_{exc} in MCH/3MP at room temperature. A figure with the $T_1 \rightarrow T_n$ absorption spectrum of *EE*-2AnPhB in cyclohexane. Supplementary figures showing plots of ln $[I_{F,2}\tau_F(293\ K)/\tau_F(T)]$ and ln $I_{F,2}/I_{F,1}$ vs $1/T$ and $I_{F,2}/I_{F,1}$ vs $[S_2]/[S_1]$ to derive $\Delta E(S_2-S_1)$ and k_{F2}/k_{F1}, respectively, for *EE*-2AnPhB in MCH/3MP. This material is available free of charge via the Internet at http://pubs.acs.org.

References and Notes

(1) (a) Allen, M. T.; Whitten, D. G. *Chem. Rev.* **1989**, *89*, 1691−1702 and references therein. (b) Saltiel, J.; Sun, Y.-P. In *Photochromism: Molecules and Systems*; Dürr, H., Bouas-Laurent, H., Eds.; Elsevier: Amsterdam, 1990; pp 64−164 and references therein.

(2) Bartocci, G.; Mazzucato, U.; Spalletti, A.; Orlandi, G.; Poggi, G. *J. Chem. Soc., Faraday Trans.* **1992**, *88*, 3139−3144 and references therein.

(3) For review articles, see: (a) Zechmeister, L. *Exper.* **1954**, *10*, 1−40. (b) Hudson, B. S.; Kohler, B. E. *Annu. Rev. Phys. Chem.* **1974**, *25*, 437−460. Hudson, B. S.; Kohler, B. E.; Schulten, K. In *Excited States*; Lim, E. C., Ed.; Academic Press: New York, 1982, Vol. 6, pp 1−95. (c) Kawski, A.; Kuklinski, B.; Kubicki, A. *Z. Naturforsch.* **1992**, *47a*, 1204−1210 and references therein. (d) Orlandi, G.; Zerbetto, F.; Zgierski, M. Z. *Chem. Rev.* **1991**, *91*, 867−891.

(4) Bensasson, R. V.; Land, E. J.; Truscott, T. G. *Excited States and Free Radicals in Biology and Medicine*; Oxford University Press: Oxford, 1993; pp 201−227.

(5) Bartocci, G.; Spalletti, A.; Becker, R. S.; Elisei, F.; Floridi, S.; Mazzucato, U. *J. Am. Chem. Soc.* **1999**, *121*, 1065.

(6) For a review article, see Mazzucato, U.; Momicchioli, F. *Chem. Rev.* **1991**, *91*, 1679−1719 and references therein.

(7) (a) Bartocci, G.; Masetti, F.; Mazzucato, U.; Spalletti, A.; Orlandi, G.; Poggi, G. *J. Chem. Soc., Faraday Trans* 2 **1988**, *84*, 385−399. Bartocci, G.; Masetti, F.; Mazzucato, U.; Baraldi, I.; Fischer, E. *J. Mol. Struct.* **1989**, *193*, 173−183. (b) Bartocci, G.; Mazzucato, U.; Spalletti, A. *Chem. Phys.* **1996**, *202*, 367−376.

(8) (a) Saltiel, J.; Zhang, Y.; Sears, D. F., Jr.; Choi, J.-O. *Res. Chem. Interm.* **1995**, *21*, 899−921. (b) Wismontski-Knittel, T.; Das, P. K.; Fisher, E. *J. Chem. Phys.* **1984**, *88*, 1163−1168. Ghiggino, K. P.; Skilton, P. F.; Fisher, E. *J. Am. Chem. Soc.* **1986**, *108*, 1146−1149. (c) Karatsu, T.; Yoshikawa, N.; Kitamura, A.; Tokumaru, K. *Chem. Lett.* **1994**, 381−384.

(9) Galiazzo, G.; Spalletti, A.; Elisei, F.; Gennari, G. *Gazz. Chim. Ital.* **1989**, *119*, 277−280.

(10) See, e.g., *Carotenoids Volume 2: Synthesis*; Britton, G., Liaaen-Jensen, S., Pfander, H., Eds.; Birkhäuser-Verlag: Basel, 1996.

(11) Bartocci, G.; Masetti, F.; Mazzucato, U.; Spalletti, A.; Baraldi, I.; Momicchioli, F. *J. Phys. Chem.* **1987**, *91*, 4733−4743. Meech, S. R.; Phillips, D. *J. Photochem.* **1983**, *23*, 193−217.

(12) Gamboni, G.; Theus, V.; Schinz, H. *Helv. Chim. Acta* **1955**, *38*, 255−263.

(13) Piantini, U.; Soresen, O. W.; Ernst, R. R. *J. Am. Chem. Soc.* **1982**, *104*, 6800−6801.

(14) Jeener, J.; Meier, B. H.; Bachmann, P.; Ernst, R. R. *J. Chem. Phys.* **1979**, *71*, 4546−4563.

(15) Macchioni, A.; Pregosin, P. S.; Engel, P. F.; Mecking, S.; Pfeffer, M.; Daran, J.-C.; Waissermann, J. *Organometallics* **1995**, *14*, 1637−1645.

(16) Neuhaus, D.; Williamson, N. *The Nuclear Overhauser Effect in Structural and Conformational Analysis*; VCH Publishers Inc.: New York 1989; p 380.

(17) Saltiel, J.; Sears, D. F., Jr.; Sun, Y.-P.; Choi, J.-O. *J. Am. Chem. Soc.* **1992**, *114*, 3607−3612.

(18) Wallace-Williams, S. E.; Moller, S.; Goldbeck, R. A.; Hanson, K. M.; Lewis, J. W.; Atom Yee, W.; Kliger, D. S. *J. Phys. Chem.* **1993**, *97*, 9587−9592.

(19) Bunker, C. E.; Lytle, C. A.; Rollins, H. W.; Sun, Y.-P. *J. Phys. Chem. A* **1997**, *101*, 3214−3221.

(20) Bartocci, G.; Mazzucato, U.; Spalletti, A.; Elisei, F. *Spectrochim. Acta* **1990**, *46A*, 413−418.

(21) Saltiel, J.; Zhang, Y.; Sears, D. F., Jr. *J. Phys. Chem. A* **1997**, *101*, 7053−7060.

(22) Itoh, T.; Kohler, B. E. *J. Phys. Chem.* **1987**, *91*, 1760−1764. Alford, P. C.; Palmer, T. F. *Chem. Phys. Lett.* **1982**, *86*, 248−253. Alford, P. C.; Palmer, T. F. *Chem. Phys. Lett.* **1986**, *127*, 19−25.

(23) Aloisi, G. G.; Elisei, F.; Latterini, L.; Mazzucato, U.; Rodgers, M. A. J. *J. Am. Chem. Soc.* **1996**, *118*, 10879−10887. Aloisi, G. G.; Elisei, F.; Latterini, L.; Marconi, G.; Mazzucato, U. *J. Photochem. Photobiol., A: Chem.* **1997**, *105*, 289−295.

(24) Wismontski-Knittel, T.; Das, P. K. *J. Phys. Chem.* **1984**, *88*, 1168−1173.

(25) Yee, W. A.; Hug, S. J.; Kliger, D. S. J. *J. Am. Chem. Soc.* **1988**, *110*, 2164−2169.

(26) Spalletti, A. et al., in preparation.

(27) Saltiel, J.; Townsend, D. E.; Sykes, A. *J. Am. Chem. Soc.* **1973**, *95*, 5968−5973.

(28) Saltiel, J.; Ko, D.-H.; Fleming, S. A. *J. Am. Chem. Soc.* **1994**, *116*, 4099−4100.

(29) Sandros, K.; Sundahl, M.; Wennerström, O.; Norinder, U. *J. Am. Chem. Soc.* **1990**, *112*, 3082−3086.

(30) Anger, I.; Sundahl, M.; Wennerström, O.; Sandros, K.; Arai, T.; Tokumaru, K. *J. Phys. Chem.* **1992**, *96*, 7027−7032.

(31) Mazzucato, U.; Spalletti, A.; Bartocci, G.; Galiazzo, G. *Coord. Chem. Rev.* **1993**, *125*, 251−260.

(32) Saltiel, J.; Zhang, Y.; Sears, D. F., Jr. *J. Am. Chem. Soc.* **1996**, *118*, 2811−2817. Saltiel, J.; Zhang, Y.; Sears, D. F., Jr. *J. Am. Chem. Soc.* **1997**, *119*, 11202−11210.

(33) (a) Velsko, S. P.; Fleming, G. R. *J. Chem. Phys.* **1982**, *76*, 3553−3562. Keery, K. M.; Fleming, G. R. *Chem. Phys. Lett.* **1982**, *93*, 322−326. (b) Kang, T. J.; Etheridge, T.; Jarzeba, W.; Barbara, P. F. *J. Phys. Chem.* **1989**, *93*, 1876−1881.

(34) Sandros, K.; Becker, H.-D. *J. Photochem. Photobiol.* **1987**, *39*, 301−315 and references therein. Sandros, K.; Becker, H.-D. *J. Photochem. Photobiol. A: Chem.* **1988**, *43*, 291−292.

(35) Arai, T.; Karatsu, T.; Misawa, H.; Kuriyama, Y.; Okamoto, H.; Hiresaki, T.; Fuuruchi, H.; Zeng, H.; Sakuragi, H.; Tokumaru, K. *Pure Appl. Chem.* **1988**, *60*, 989−998. Tokumaru, K.; Arai, T. *J. Photochem. Photobiol. A: Chem.* **1992**, *65*, 1−13. Arai, T.; Tokumaru, K. *Chem. Rev.* **1993**, *93*, 23−39 and references therein.

(36) Karatsu, T.; Kitamura, A.; Zeng, H.; Arai, T.; Sakuragi, H.; Tokumaru, K. *Bull. Chem. Soc. Jpn.* **1995**, *68*, 920−928.

(37) Bartocci, G.; Spalletti, A.; Mazzucato, U. *Res. Chem. Interm.* **1995**, *21*, 735−747.

(38) Spalletti, A.; Bartocci, G.; Elisei, F.; Mancini, V.; Mazzucato, U. *J. Chem. Soc., Faraday Trans.* **1997**, *93*, 211−219.

(39) Hug, G.; Becker, R. S. *J. Chem Phys.* **1976**, *65*, 55−63.

(40) Birnbaum, D.; Kohler, B. E.; Spangler, C. W. *J. Chem. Phys.* **1991**, *94*, 1684−1691.

(41) Birks, J. B. In *Photophysics of Aromatic Molecules*; Wiley-Interscience: New York, 1970; p 88, eq 4.22.